Nonradiative recombination in 1.56μm GaInNAsSb/GaNAs quantum-well lasers

J. W. Ferguson, P. M. Smowton, P. Blood, H. Bae, T. Sarmiento et al.

Citation: Appl. Phys. Lett. **95**, 231104 (2009); doi: 10.1063/1.3271182
View online: http://dx.doi.org/10.1063/1.3271182
View Table of Contents: http://apl.aip.org/resource/1/APPLAB/v95/i23
Published by the American Institute of Physics.

Nonradiative recombination in 1.56 μm GaInNAsSb/GaNAs quantum-well lasers

J. W. Ferguson,[1,a)] P. M. Smowton,[1] P. Blood,[1] H. Bae,[2] T. Sarmiento,[2] and J. S. Harris, Jr.[2]
[1]*Cardiff School of Physics and Astronomy, Cardiff University, Queens Buildings, Cardiff CF24 3AA, United Kingdom*
[2]*Solid State and Photonics Laboratory, Stanford University, Stanford, California 94305, USA*

(Received 18 August 2009; accepted 12 November 2009; published online 8 December 2009)

We have shown experimentally that in GaInNAsSb/GaAs quantum-well lasers there are significant nonradiative contributions to threshold current from the barriers and the well. By matching a simulation to the experiment we find that Auger recombination in the barriers is very weak, due to the low carrier density. Shockley–Read–Hall recombination is the dominant source of nonradiative current, with the barriers making the major contribution, possibly due to their higher defect density than the wells. This suggests that significant improvements could be made by optimizing growth conditions and layer design, with particular attention to the barrier. © *2009 American Institute of Physics*. [doi:10.1063/1.3271182]

GaInNAsSb quantum-well (QW) lasers on GaAs substrates have recently been developed with room temperature threshold current densities of 318 A cm^{-2} and 1.54 μm emission.[1] However, a number of mechanisms still limit performance including nonradiative defect-related (Shockley–Read–Hall) (SRH) recombination and Auger recombination. In this work we identify experimentally the contribution the barriers and the wells make to the nonradiative current in state of the art GaInNAsSb/GaNAs lasers and use a simulation to identify the likely source of this nonradiative current. From measurement of the radiative current density we also identify the ultimate performance if the nonradiative processes can be removed.

The samples were grown using molecular beam epitaxy and contain 7 nm wide GaInNAsSb QWs within GaNAs barriers. There are four designs, with either one or three QWs and two different Nitrogen contents in the well, 3% and 3.3% N. The single well structure has 20 nm wide barriers of GaNAs and the three well structure has 20 nm barriers of GaNAs between each well. Details of the growth of similar structures has been published.[1] After growth, the lasers were annealed at 680 °C for 10 min in a rapid thermal annealer furnace using a GaAs proximity cap to minimize arsenic desorption. The material was processed into multimode devices that are 1500 μm long and 300 μm wide, with a 50 μm oxide stripe running down the center. This top contact of the device was then split into 300 μm long electrically isolated sections.

The device characteristics were measured using the segmented contact technique.[2] This is a single pass measurement which produces modal gain, absorption, and spontaneous emission rate spectra as a function of photon energy. The calibrated spontaneous emission rate spectra give the current density associated with spontaneous recombination.[2] The measurements are performed pulsed, at a temperature of 300 K, and with a polarizer in place set to TE, (there is no significant TM emission from these samples). To enable us to compare results for different samples at the same level of pumping, we determined the difference between the quasi Fermi level separation and the effective band gap of the QW system using a reference absorption edge (AE) energy obtained from the absorption spectrum and the transparency point (TP) obtained from the gain spectrum, for a given current density. Figure 1 shows gain and absorption spectra and marks where the reference AE energy and TP are taken. The reference AE energy is defined as the value of photon energy at which the modal absorption spectrum is equal to 50 (1 well) or 150 cm^{-1} (3 well) as we expect the modal absorption and modal gain of the three well structure to be three times that of the single well structure due to the differences in total optical confinement factor.

The measured absorption spectra (not shown) show a shift in AE between the 3% and 3.3% nitrogen contents of 17 meV for the one well structures and 12 meV for the three well structures. This suggests first that the nitrogen content may not be the same in the one and three well samples and second that the difference between the nitrogen contents in these samples may not be as large as intended since a 30 meV band-edge shift is expected for 0.3% nitrogen difference in InGaAsN samples.[3] The shape of the absorption spectra, and specifically the AE, is the same for all the samples indicating the same level of inhomogeneous broadening for all samples.

When the modal gain per well is plotted against the radiative current density per well (Fig. 2), the samples containing the same amount of nitrogen (but different numbers of

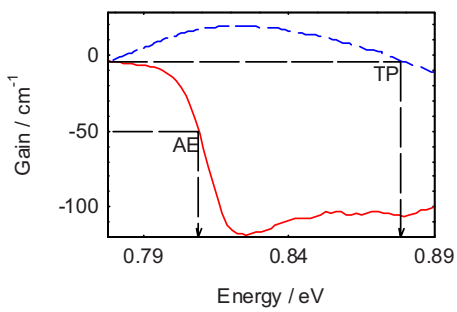

FIG. 1. (Color online) Typical absorption and gain spectra with the TP marked on the dashed gain line and the AE marked on the solid absorption curve.

a)Electronic addresses: fergusonjw@cf.ac.uk and fergusonjw@cardiff.ac.uk.

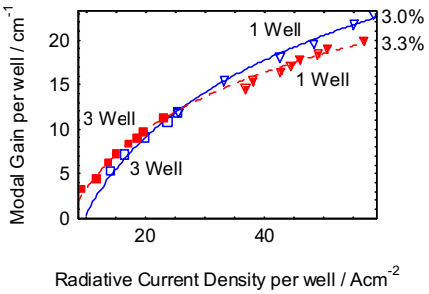

FIG. 2. (Color online) Modal gain per well plotted against radiative current density per well. The triangles are the one well samples, the squares are the three well. The open symbols and the closed symbols are the 3% and 3.3% nitrogen samples, respectively.

wells) are described by the equation $G=G_0 \ln(J/J_t)$,[4] using the same values of G_0 and J_t. This is consistent with each well in the three well samples and the one well samples being equally populated and the optical confinement factor being the same for each well, as was assumed in the treatment of the AE above. The higher nitrogen content results in a slightly lower transparency current density (J_t) 7.1 A cm^{-2} compared to 9.7 A cm^{-2} and a lower gain parameter (G_0) 9.5 cm^{-1} compared to 12.5 cm^{-1}.

We can determine the total nonradiative current by subtracting the radiative current density, given by the calibrated spontaneous emission spectra, from the total applied current density. This nonradiative current density is plotted against TP minus AE in Fig. 3 and the data forms two distinct groups of points dependent on well number but not nominal nitrogen content.

From the data of Fig. 2, we assume that the barriers and the wells are the same in all the samples and we also assume that there is negligible leakage into the cladding layers due to the large band offsets between well and cladding (0.52 eV in the conduction band and 0.18 eV in the valence band). We represent the nonradiative current density in one well by W and in one barrier by B. The nonradiative current in the one well sample is $J_{nr}(1)=(1W+2B)$ and in the three well sample $J_{nr}(3)=(3W+4B)$. If these currents are determined by the level of pumping, at fixed TP minus AE the nonradiative current density in one barrier (B) and one well (W) can be derived by simple algebra, for example

$$B = \frac{3^*[J_{nr}(1)] - [J_{nr}(3)]}{2}. \quad (1)$$

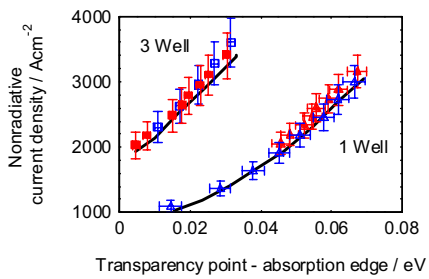

FIG. 3. (Color online) Plot of the nonradiative current density against TP minus AE. The triangles are the one well samples the squares are the three well. The open symbols and the closed symbols are the 3% and 3.3% nitrogen samples, respectively. The solid black lines are the results of the simulation.

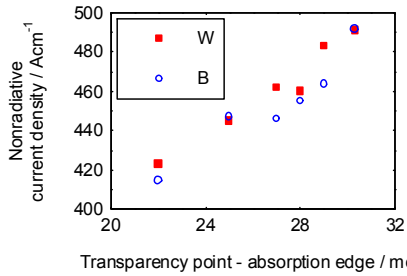

FIG. 4. (Color online) Nonradiative current density per barrier (open circles) and per well (closed squares) as a function of transparency minus AE.

The values of nonradiative recombination for one barrier and one well are plotted against TP minus AE in Fig. 4 over the range where data for both one and three well samples exist. This shows that the nonradiative contribution from one barrier is of a similar magnitude to the contribution from one well therefore for a single well system the two barriers contribute two thirds of the nonradiative current. For a thermal carrier distribution the carrier density in the barrier should be lower than in the QWs but the barriers are three times wider than the well and contain 30%–40% more nitrogen and may therefore have a higher defect concentration.

We use the simulation program SIMWINDOWS (Ref. 5) to identify the processes involved in the nonradiative recombination and their relative strengths. SIMWINDOWS is a one dimensional Schrodinger, Poisson, continuity equation solver using Fermi statistics, which has previously been used to analyze vertical cavity surface emitting lasers[6] and InGaN LED structures.[7] The input parameters used were mainly taken from the literature and are given in Table I.

To compare the model with experimental data the value of quasi-Fermi level separation in the simulation was set to the experimental value for a particular current density. The radiative recombination constant was then adjusted until the radiative current density agreed with the experimental value. The value of the Auger coefficient was kept the same in the well and the barrier and was taken from literature. Since the well and barrier may contain different concentrations of defects and impurities the values of the SRH coefficients in the well and barrier were adjusted until the total current densities

TABLE I. The input parameters used in the SIMWINDOWS simulations.

Parameter	Value
GaInNAsSb electron mass	0.137 m_0 [a]
GaAsN electron mass	0.102 m_0 [a]
GaInNAsSb hole mass	0.44 m_0 [a]
GaAsN hole mass	0.385 m_0 [a]
QW radiative recombination co-efficient (cm^2 s^{-1})	3.5×10^{-5}
QW SRH lifetime (ns)	0.5
QW Auger co-efficient (cm^4 s^{-1})	3.5×10^{-17} [b]
Barrier SRH lifetime (ns)	0.0265
Barrier Auger co-efficient (cm^6 s^{-1})	3.5×10^{-29} [b]
GaInNAsSb band gap (eV)	0.725[c]
GaInNAsSb electron affinity	4.391[c]
GaAsN band gap (eV)	0.95[c]
GaAsN affinity	4.22[c]

[a]Reference 9.
[b]Reference 10.
[c]Reference 1.

TABLE II. Magnitude of the contributions to the current densities of each process obtained from the simulation.

	In a well (A cm^{-2})	In a barrier (A cm^{-2})
Auger recombination	106	0.02
SRH recombination	336	442
Radiative recombination	24.9	0.08

were the same as were found experimentally. The current densities associated with radiative, Auger, and SRH recombination both in the well and the barrier at a TP minus AE of 0.025 eV, are shown in Table II. For the one well sample the total Auger current predicted is 106 A cm^{-2}, and the total SRH current predicted is 1220 A cm^{-2} suggesting that, overall, SRH recombination is the major nonradiative process. In the simulation the value of SRH lifetime in the barriers is about 20 times shorter than in the well, suggesting a higher defect concentration.

Since Auger recombination is proportional to the Auger coefficient we can see from Table II, that Auger recombination in the barrier will not make a significant contribution to the nonradiative current unless an Auger coefficient 10 000 times larger is used. Furthermore, since the total current density is defined by the experiment the Auger coefficient in the well would then, at maximum, be 1000 times smaller than that used in the barrier. Given the similarities in the well and barrier material a large difference in Auger coefficients is not physically reasonable. We suppose that the small simulated Auger current in the barrier arises from the low carrier density.

To further test the simulation, the value of transparency point minus absorption edge or TP minus AE was changed in the model to cover a range of values common to the one and three well structures. The simulated lines shown in Fig. 3, are in good agreement with experiment using the same parameters as in Table I.

The data from Fig. 2 shows that if all nonradiative recombination could be removed using a combination of changes in growth and layer design, for a laser of length 1 mm with uncoated facets having an optical loss of 17 cm^{-1} (α_i=5 cm^{-1}), the radiative threshold current density is 35 A cm^{-2} for a single well. This is similar to quantum dot lasers emitting at 1.3 μm, where the saturated gain is also relatively low.[8] However, Auger recombination may not be easily eliminated and SIMWINDOWS predicts that if SRH recombination is removed, for the same laser, the threshold current density is 320 A cm^{-2}

In summary, we have quantified the nonradiative current density of GaInNAsSb/GaAs QW lasers and have shown that the nonradiative currents are similar in a single barrier and a single well. Using the simulation SIMWINDOWS, we have shown that Auger recombination in the barriers is very weak, due to the low carrier density. SRH recombination is the dominant source of nonradiative current, with the barriers making the major contribution, possibly due to their higher defect density than the wells. This suggests that significant improvements could be made by a combination of optimizing growth conditions and layer design, with particular attention to the barrier.

OCLARO Inc. and EPSRC under Grant No. EP/F006683, are thanked for funding.

[1]S. R. Bank, H. Bae, L. L. Goddard, H. B. Yuen, M. A. Wistey, R. Kudrawiec, and J. S. Harris, IEEE J. Quantum Electron. **43**, 773 (2007).
[2]P. Blood, G. M. Lewis, P. M. Smowton, H. Summers, J. Thomson, and J. Lutti, IEEE J. Sel. Top. Quantum Electron. **9**, 1275 (2003).
[3]M. Weyers, M. Sato, and H. Ando, Appl. Phys. (Berlin) **31**, 853 (1992).
[4]L. A. Coldren and S. W. Corzine, in *Diode Lasers and Photonics Integrated Circuits*, Series in Microwave and Optical engineering Vol. 1, edited by K. Chang (Wiley, New York, 1995).
[5]SIMWINDOWS home page http://www.ocs.colorado.edu/SimWindows/simwin.html.
[6]D. W. Winston and R. E. Hayes, IEEE J. Quantum Electron. **34**, 707 (1998).
[7]J. D. Thomson, I. A. Pope, P. M. Smowton, P. Blood, R. J. Lynch, G. Hill, T. Wang, and P. Parbrook, J. Appl. Phys. **99**, 024507 (2006).
[8]I. O'Driscoll, P. M. Smowton, and P. Blood, IEEE J. Quantum Electron. **45**, 380 (2009).
[9]L. L. Goddard, S. R. Bank, M. A. Wistey, H. B. Yuen, Z. Rao, and J. S. Harries, Jr., J. Appl. Phys. **97**, 083101 (2005).
[10]H.-F. Liu and W. F. Ngai, IEEE J. Quantum Electron. **29**, 1668 (1993).